

Instabilities of the Conventional Nucleus-Nucleus Interactions for (^3H , ^4He) Proton Pickup Cross-Sections

A. A. Farra¹

Received March 21, 2005; accepted January 24, 2006

Published Online: February 27, 2007

The angular distributions of the ^{26}Mg , ^{28}Si , ^{30}Si (^3H , ^4He) reactions have been analyzed using the exact finite-range DWBA calculations. The optical model potential is assumed to have the conventional spin-orbit potential. The obtained cross-sections with the spin-orbit potential are not significantly different from those calculated using the phenomenological Woods-Saxon form factors in the forward angle regions. The inclusion of the spin-orbit potential gives the best fit to the data and greatly improves the large angle cross-sections. Different reasonable spectroscopic factors are found to account well for the cross-section magnitudes.

KEY WORDS: instabilities of the conventional nucleus; nucleus interactions for (^3H , ^4He) proton; pickup cross-sections.

1. INTRODUCTION

The (α , d) reactions have been studied at different incident energies in terms of the DWBA analysis using the best available shell-model wave functions (Davis and Nelson, 1986; Skwirczynska *et al.*, 1981). Interestingly, the (^3He , d) angular distribution (Yasue *et al.*, 1993) have been studied to investigate the microscopic two-nucleon configuration for the 6^- states as well as to identify the J^π values. The microscopic DWBA analysis including a modified delta interaction has been used to investigate the structure of low-lying states for the ^{60}Ni , ^{62}Ni (^3He , p) reactions (Haque *et al.*, 1998; Sen Gupta *et al.*, 1990). In such calculations, the calculated cross-sections for the ^{26}Mg (^3He , n) ^{28}Si reaction were found in good agreement with the experimental data (Abe *et al.*, 1987) using the one-step DWBA calculations.

In the present work, the differential cross-sections of various proton pickup reactions have been calculated using different optical potentials. In Section 2,

¹ Physics Department, Faculty of Science, Al-Azhar University, P. O. Box 1277, Gaza, Palestine;
e-mail: a_a_farra@hotmail.com

only outline of the reaction form factor is introduced. The analysis of angular distributions is summarized in Section 3. Section 4 is left for discussion and conclusion.

2. REACTION FORM FACTOR

In an effort to find a more consistent analysis of the data, we have performed the DWBA calculations following the exact finite range (Osman and Farra, 1989; Osman and Farra, 1994). It is therefore, the transition amplitude of the $A(a,b)B$ pickup reaction is given as

$$T_{fi} = \iint dr_a dr_b \chi_b^{*(-)}(r_b) \langle Bb | V | Aa \rangle \chi_a^{(+)}(r_a) \quad (1)$$

where $\chi^{(+)}$ and $\chi^{(-)}$ are the in going and out going distorted waves, respectively. Here $\langle Bb | V | Aa \rangle$ stands for the effective nucleus–nucleus interaction. Throughout the present analysis, the particle–particle binding interactions are assumed to have the Hulthen potential

$$V_{np}(r) = -V_1 e^{-\alpha_H r} [1 - e^{-\alpha_H r}]^{-1} + V_2 e^{-\beta_H r} [1 - e^{-\beta_H r}]^{-1} \quad (2)$$

where V_1 and V_2 are the potential strengths, while, α_H and β_H denote their decay factors. The potential parameters are adjusted to have $V_1 = 149.3$ MeV, $V_2 = 402.9$ MeV, $\alpha_H = 1.48$ fm $^{-1}$ and $\beta_H = 5.64$ fm $^{-1}$. In these calculations, the bound state wave function is described by

$$\Phi(r) = N_H e^{-\gamma_H r} (1 - e^{-\alpha_i r}); \quad i = 1, 2 \quad (3)$$

where N_H is the Hulthen normalization factor given as

$$N_H = \left(\frac{2\gamma_H (\gamma_H + \alpha_H) (2\gamma_H + \alpha_H)}{\alpha_H^2} \right)^{\frac{1}{2}} \quad (4)$$

with

$$\gamma_H = \left(\frac{ME_d}{\hbar^2} \right)^{\frac{1}{2}} \quad (5)$$

Here, M and E_d are the reduced mass and the binding energy, respectively.

3. ANALYSIS OF ANGULAR DISTRIBUTIONS

In the present analysis, initially the differential cross-section of the ^{26}Mg , ^{28}Si , $^{30}\text{Si}(^3\text{H}, ^4\text{He})$ reactions have been calculated using standard Woods–Saxon optical model potential. In these calculations, the six- Woods–Saxon potential parameters are varied to give the best fit of the data by minimizing χ^2 . The obtained parameters (set I) are given in Table I and the corresponding results are

Table I. Optical Potential Parameters Used in the DWBA Calculations

Channel	Set	V (MeV)	r_o (fm)	a (fm)	W_V (MeV)	W_D (MeV)	r_I (fm)	a_I	$V_{S.O.}$	$r_{S.O.}$ (fm)	$a_{S.O.}$ (fm)	r_C (fm)
$^3\text{H} + ^{26}\text{Mg}$	I	185.7	1.38	0.58	25.60	1.21	0.67	1.20	1.290	0.65	1.25	
	II	217.6	1.15	0.62		37.21	1.31	0.85				1.40
$^3\text{H} + ^{28,30}\text{Si}$	I	76.0	1.28	0.67	18.6	1.15	0.58	1.26	5.09	1.20	0.35	1.25
	II	69.0	1.23	0.74	2.97	11.02	1.26					1.25
$^4\text{He} + ^{25}\text{Na}$	I	79.6	1.35	0.58	13.2	1.35	0.58	1.32	0.74	6.49	1.07	1.30
	II	84.0	1.17	0.75	1.1	11.9	1.32					1.30
$^4\text{He} + ^{27,29}\text{Al}$	I	76.0	1.31	0.63	23.0	1.28	0.54	1.20	1.20	0.66	1.40	1.40
	II	49.0	1.70	0.57	1.1	7.34	1.38					1.40
(p, n)		<u>\underline{a}</u>	1.25	0.65		2.5^b	1.25			0.65		1.40

^a Adjusted to reproduce the binding energies.^b $\lambda = 25$.

shown in Figs. 1–3 by dashed lines. In fact, the resulting potential parameters are found to be not drastically different from those used to start searches and the fits to the data are quite good over the entire angular range. For these calculations, the form factor of the transferred nucleon was calculated using the usual separation energy method in a Woods-Saxon well of radius $r_o = 1.25$ fm and diffuseness $a = 0.65$ fm. In addition, a second set of calculation has been performed using the spin-orbit potential (Sen Gupta *et al.*, 1990). The optical potential used was of the form

$$\begin{aligned} V(r) = & -Vf(r, r_a, a) - i \left[W_V - 4a_I W_D \frac{d}{dr} \right] f(r, r_I, a) \\ & + \left(\frac{\hbar}{m_\pi c} \right)^2 V_{\text{S.O.}} \frac{1}{r} \frac{d}{dr} f(r, r_{\text{S.O.}}, a_{\text{S.O.}}) + V^C(r) \end{aligned} \quad (6)$$

with

$$f(r) = [1 + \exp\{(r - r_o A^{1/3})/a\}]^{-1} \quad (7)$$

where $V^C(r)$ is the Coulomb potential of a uniform charged sphere of radius $r_c A^{1/3}$. The obtained results of the differential cross-sections are displayed by solid curves in Figs. 1–3. It is found that the fits with potential parameters set II reproduce quite well the shape and magnitude of the cross-sections. Where the calculations including the spin orbit term lead to better descriptions of the large angle data than those using the phenomenological Woods-Saxon potential. Throughout the present calculations, the spectroscopic factor for each transfer process is extracted from Vernotte *et al.* (1993)

$$\left(\frac{d\sigma(\theta)}{d\Omega} \right)_{\text{exp}} = N \frac{C^2 S_{lj}}{2j+1} \left(\frac{d\sigma(\theta)}{d\Omega} \right)_{\text{theor}} \quad (8)$$

where N stands for the normalization factor and S_{lj} is the spectroscopic factor for the transfer of a single nucleon of orbital angular momentum l and total angular momentum $j \cdot C^2$ is the isospin Clebsch-Gordan coefficient. The obtained spectroscopic factors are listed in Table II.

4. DISCUSSION AND CONCLUSION

In the present work, the angular distributions for the ^{26}Mg , ^{28}Si , ^{30}Si (^3H , ^4He) proton pickup reactions have been successfully described in terms of the EFR-DWBA calculations using different optical model potentials. From the results shown in Figs. 1–3, the present calculations using spin-orbit potential gives the best fit to the data and greatly improve the large angle cross-sections. Where the forward regions are found to be insensitive to the optical potential. Generally, it

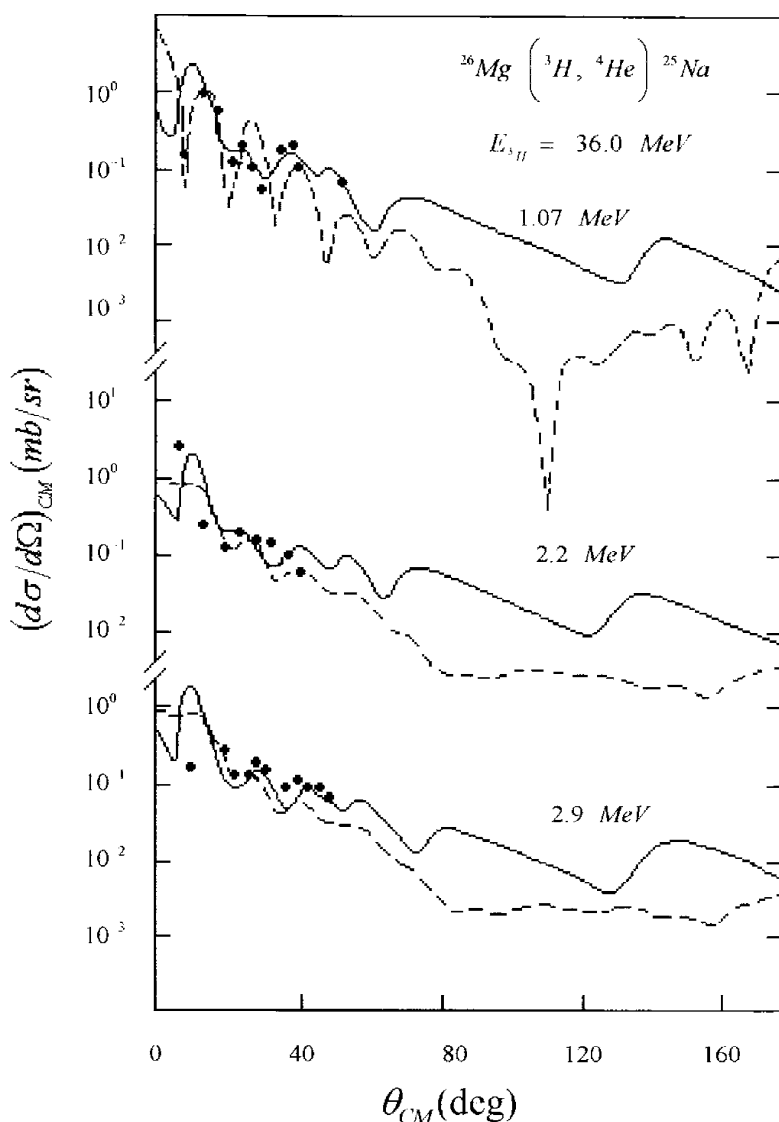


Fig. 1. Differential cross-sections of the $^{26}\text{Mg}(^3\text{H}, ^4\text{He})^{25}\text{Na}$ reaction at 36.0 MeV. The solid and dashed curves are the present DWBA calculations using spin-orbit potential set II and Woods-Saxon potential set I, respectively. The experimental data are taken from reference Pearce *et al.* (1987).

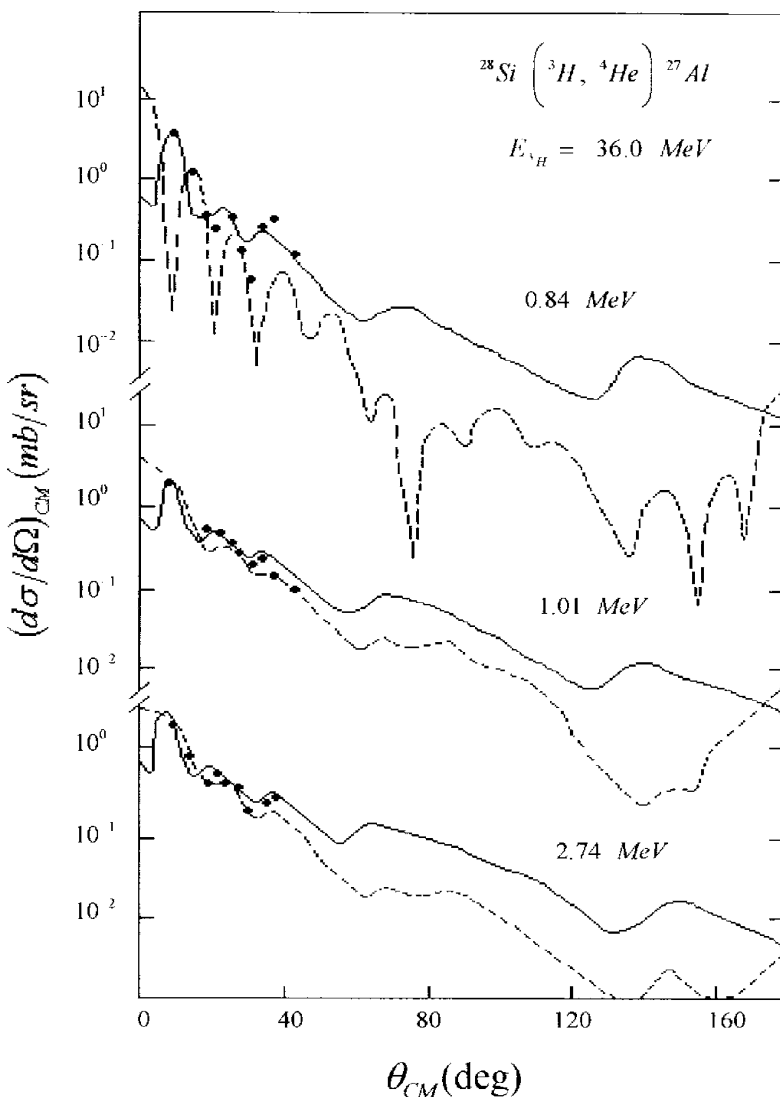


Fig. 2. The same as Fig. 1 except for the $^{28}Si(^3H, ^4He)^{27}Al$ reaction. The data are from reference Pearce *et al.* (1987).

is found that more than one potential parameter sets give equally good fits to the data in the forward regions. Where the calculated cross-sections with potential parameter set I found close enough to those obtained within set II in the forward regions. In view of comparison, the present calculations using spin-orbit potential

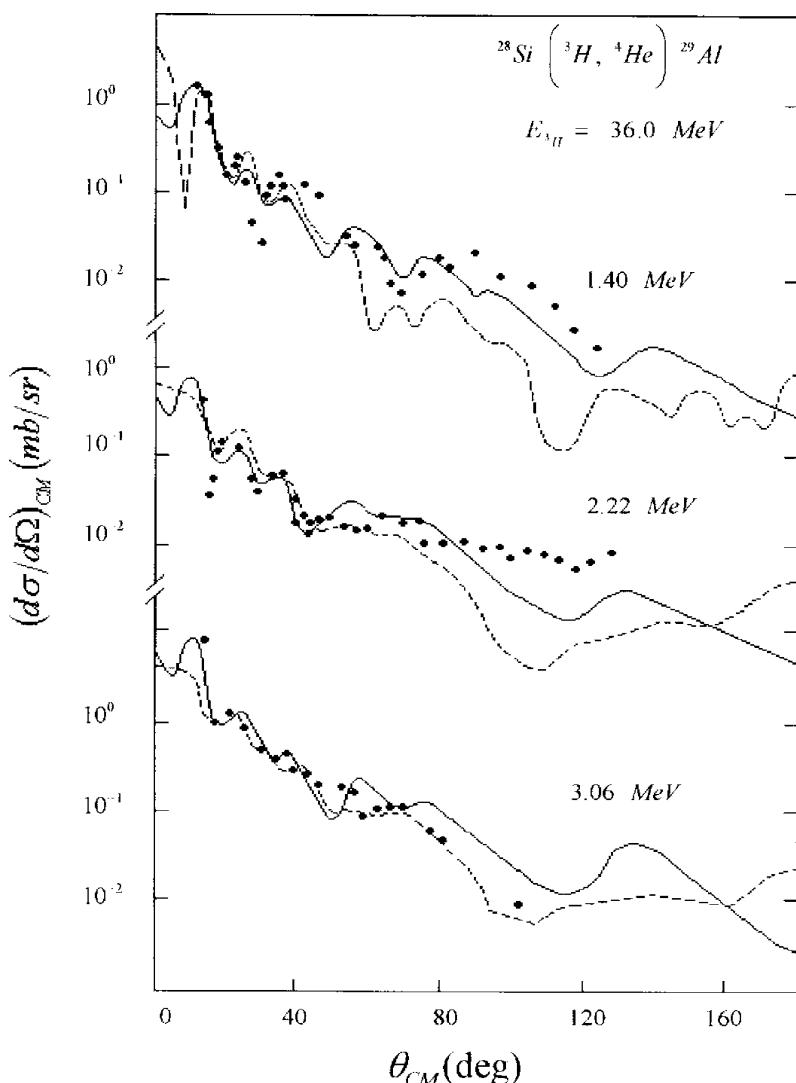


Fig. 3. The same as Fig. 1 except for the $^{30}\text{Si}(^3\text{H}, ^4\text{He})^{29}\text{Al}$ reaction. The data are from reference Pearce *et al.* (1987).

introduce a better description of the data than earlier calculations (Pearce *et al.*, 1987). In addition, the Hulthen-form factor has led to similar results as those obtained with Yukawa potential (Osman and Farra, 1989) and slightly different from those using Gaussian potential (Vernotte *et al.*, 1993). In fact, different values of normalization and spectroscopic factors are found to be reasonable to

Table II. Spectroscopic Factors

Reaction	Incident energy (MeV)	Excitation energy (MeV)	J^π	Spectroscopic factors			
				Previous		Present	
				FR	ZR	WS	S.O.
$^{26}\text{Mg}(^3\text{H}, ^4\text{He})^{25}\text{Na}$	36.0	1.07	$\frac{1}{2}^+$	0.08	0.12	0.63	0.69
		2.20	$\frac{3}{2}^+$	0.14	0.20	0.67	0.71
		2.91	$\frac{5}{2}^+$	0.14	0.19	0.66	0.70
$^{28}\text{Si}(^3\text{H}, ^4\text{He})^{27}\text{Al}$	36.0	1.07	$\frac{1}{2}^+$	0.36	0.68	0.59	0.76
		1.01	$\frac{3}{2}^+$	0.70	0.78	0.75	0.77
		2.74	$\frac{5}{2}^+$	0.60	0.44	0.78	0.85
$^{28}\text{Si}(^3\text{H}, ^4\text{He})^{29}\text{Al}$	36.0	1.40	$\frac{1}{2}^+$	0.23	0.22	0.61	0.82
		2.22	$\frac{3}{2}^+$	0.11	0.11	0.73	0.79
		3.06	$\frac{5}{2}^+$	0.76	0.59	0.67	0.74

account well for the cross-sections. Where the best fits to the data obtained with normalization of range $N = 15\text{--}20 \times 10^4 \text{ MeV}^2 \text{ fm}^3$.

In conclusion, the present DWBA calculations using spin-orbit optical potential give the best overall fit to the data and are found to be appropriate to describe the mean feature of the differential cross-sections for the most considered systems. The most significant conclusion is that the spin-orbit and the phenomenological Woods–Saxon potentials provide quite similar results to the forward angle cross-sections of the various ($^3\text{H}, ^4\text{He}$) data at low energy.

REFERENCES

- Abe, K., Maeda, K., Ishimatsu, T., Kawamura, T., Furukawa, T., Orithara, H., and Zafiratos, C. D. (1987). *Nuclear Physics A* **462**, 358.
- Davis, N. J. and Nelson, J. M. (1986). *Nuclear Physics A* **458**, 475.
- Haque, M., Das, S. K., Basak, A. K., and Sen Gupta, H. M. (1998). *IL Nuovo Cimento* **111A**, 1131.
- Osman, A. and Farra, A. A. (1989). *Journal of Physics G: Nuclear and Particle Physics* **15**, 871.
- Osman, A. and Farra, A. A. (1994). *IL Nuovo Cimento* **107A**, 207.
- Pearce, K. I., Clarke, N. M., Griffiths, R. J., Simmonds, P. J., Barker, J. B. A., England, Mannion, M. C., and Ogilvie, C. A. (1987). *Nuclear Physics A* **467**, 215.
- Sen Gupta, H. M., England, J. B. A., Khazaie, F., E-Rawas, E. M., and Squier, G. T. A. (1990). *Nuclear Physics A* **517**, 82.
- Skwirczynska, I., Kozik, E., Budzanowski, A., Ploskonka, J., and Strzalkowskl, A. (1981). *Nuclear Physics A* **371**, 288.
- Vernotte, J., Berrier-Ronsin, G., Fortier, S., Hourani, E., Kalifa, J., Maison, J. M., Rosier, L. H., Rotbard, G., and Wildenthal, B. H. (1993). *Physical Review C* **48**, 205.
- Yasue, M., Sato, H., Tanaka, M. H., Hasegawa, T., Tanabe, T., Nisimura, K., Hohnuma, Shimizu, H., Ieki, K., Toyokawa, H., Hayakawa, S. I., Ogawa, K., Kadota, Y., and Peterson, R. J. (1993). *Nuclear Physics A* **563**, 457.